# 125 GeV Higgs state in the context of four generations with two Higgs doublets

Michael Geller,[1,*] Shaouly Bar-Shalom,[1,†] Gad Eilam,[1,2,‡] and Amarjit Soni[3,§]

[1]*Physics Department, Technion-Institute of Technology, Haifa 32000, Israel*
[2]*Center for High Energy Physics, Indian Institute of Science, Bangalore 500 012, India*
[3]*Theory Group, Brookhaven National Laboratory, Upton, New York 11973, USA*

(Received 26 September 2012; published 4 December 2012)

We interpret the recent discovery of a 125 GeV Higgs-like state in the context of a two-Higgs-doublet model with a heavy fourth sequential generation of fermions, in which one Higgs doublet couples only to the fourth-generation fermions, while the second doublet couples to the lighter fermions of the first three families. This model is designed to accommodate the apparent heaviness of the fourth-generation fermions and to effectively address the low-energy phenomenology of a dynamical electroweak-symmetry-breaking scenario. The physical Higgs states of the model are, therefore, viewed as composites primarily of the fourth-generation fermions. We find that the lightest Higgs, $h$, is a good candidate for the recently discovered 125 GeV spin-zero particle, when $\tan\beta \sim \mathcal{O}(1)$, for typical fourth-generation fermion masses of $M_{4G} = 400$–$600$ GeV, and with a large $t$-$t'$ mixing in the right-handed quark sector. This, in turn, leads to $\mathrm{BR}(t' \to th) \sim \mathcal{O}(1)$, which drastically changes the $t'$ decay pattern. We also find that, based on the current Higgs data, this two-Higgs-doublet model generically predicts an enhanced production rate (compared to the Standard Model) in the $pp \to h \to \tau\tau$ channel, and reduced rates in the $VV \to h \to \gamma\gamma$ and $p\bar{p}/pp \to V \to hV \to Vbb$ channels. Finally, the heavier $CP$-even Higgs is excluded by the current data up to $m_H \sim 500$ GeV, while the pseudoscalar state, $A$, can be as light as 130 GeV. These heavier Higgs states and the expected deviations from the Standard Model din some of the Higgs production channels can be further excluded or discovered with more data.

DOI: 10.1103/PhysRevD.86.115008 PACS numbers: 12.60.−i, 12.60.Fr

## I. INTRODUCTION

The LHC has recently observed a new scalar particle with a mass around ~125 GeV that could be consistent with the Higgs boson of the Standard Model (SM) [1,2]. In addition, a study of the combined Tevatron data has revealed a smaller broad excess corresponding to a mass between 115 GeV and 135 GeV [3], which is consistent with this LHC discovery. With more data collected, the LHC is expected to be able to unveil the detailed properties of the new scalar particle and verify its nature.

From the theoretical side, there has been a collective effort in the past decades in the search for new physics, beyond the SM, that can address some of the fundamental unresolved questions in particle physics. One simple candidate that was extensively studied in the past several years is the so-called SM4 (also referred to as "naive" or "simple" SM4), the SM with a fourth sequential generation of fermions (for reviews, see Refs. [4–7]). This simple extension of the SM was studied for addressing some of the challenges in particle physics, such as the hierarchy problem [8–11], the origin of the matter-antimatter asymmetry in the Universe [12,13], the apparent anomalies in flavor physics [14–18] and other issues [19].

Unfortunately, the recent LHC searches for the SM4 heavy fourth-generation quarks have now pushed the exclusion limits to ~550 GeV for the $t'$ and ~600 GeV for the $b'$ [20], which is on the border of their perturbative regime. Moreover, the SM4 Higgs was already excluded in the mass range 120–600 GeV by the 2011 data [21] when $m_{\nu_4} > m_h/2$. Thus, the above reported discovery of a light Higgs with a mass around 125 GeV is not compatible with the SM4, which includes a heavy fourth-generation neutrino with a mass $m_{\nu_4} \gtrsim 100$ GeV; i.e., with a mass larger than the current lower bound on $m_{\nu_4}$ [22]. In fact, it was further pointed out recently in Refs. [23–26] that the interpretation of the measured Higgs signals is not consistent with the SM4 either for the case $m_{\nu_4} < m_h/2$. In particular, in the SM4, the leading gluon fusion light-Higgs production mechanism is enhanced by a factor of ~10 due to the contribution of diagrams with $t'$ and $b'$ in the loops [27], which in general leads to larger signals (than what was observed at the LHC) in the $h \to ZZ/WW/\tau\tau$ channels. However, if the fourth-generation masses are of $\mathcal{O}(600)$ GeV, then the decay channels $h \to ZZ/WW$ are suppressed due to next-to-leading-order (NLO) corrections [28,29], and the exclusion of the SM4 is based mainly on the $\tau\tau$ channel. In the $h \to \gamma\gamma$ channel, there is also a substantial suppression of $\mathcal{O}(0.1)$ due to (accidental) destructive interference in the loops [27,30] and another $\mathcal{O}(0.1)$ factor due to NLO corrections [28,29]. When $\nu_4$ is taken to be light enough so that $\mathrm{Br}(h \to \nu_4\nu_4)$ becomes $\mathcal{O}(1)$, then the $\gamma\gamma$ channel becomes further

*mic.geller@gmail.com
†shaouly@physics.technion.ac.il
‡eilam@physics.technion.ac.il
§soni@bnl.gov

 

suppressed to the level that the observed excess can no longer be accounted for [24]. For a recent comprehensive analysis of the SM4 status in light of the latest Higgs results and electroweak precision data (EWPD), we refer the reader to Ref. [31].

However, as was noted already twenty years ago [32], and more recently in Refs. [33,34], if heavy fourth-generation fermions are viewed as the agents of electroweak symmetry breaking (and are, therefore, linked to strong dynamics at the nearby TeV scale), then more Higgs particles are expected at the sub-TeV regime. In this case, the Higgs particles may be composites of the fourth-generation fermions, and the low-energy composite Higgs sector should resemble a two- (or more) Higgs-doublet framework. Indeed, the phenomenology of multi-Higgs fourth-generation models was studied recently in Refs. [33–48], and within a SUSY framework in Refs. [13,49–51]; for a review, see Ref. [52]. In Ref. [53], it was also shown that the current exclusion limits on the SM4 $t'$ and $b'$ could be significantly relaxed if the four-generation scenario is embedded in a two Higgs doublet model (2HDM) framework.

Adopting this viewpoint—i.e., that the fourth-generation setup should be more adequately described within a multi-Higgs framework—we will study in this paper the expected Higgs signals of a 2HDM with a fourth-generation family, investigating whether the interpretation of the recently measured 125 GeV Higgs properties are consistent with one of the neutral scalars of the fourth-generation 2HDM.

## II. 2HDMS AND FOURTH-GENERATION FERMIONS

The 2HDM structure has the inherent freedom of choosing which doublet couples to which fermions. For the three-generation 2HDM, three popular setups have been suggested, and these are usually referred to as type-I, type-II, and type-III 2HDMs. In the case where the 2HDM is assumed to underlie some form of TeV-scale strong dynamics mediated by the fourth-generation fermions, we expect the Higgs composites to couple differently to the fourth-generation fermions. This can be realized in a class of 2HDM models named the 4G2HDMs, suggested in Ref. [34]. Most of our analysis below is performed in this 4G2HDM framework, and a comparison to a 2HDM of type II (which also underlies the SUSY Higgs sector) with and without a fourth-generation will also be discussed.

Let us recapitulate the salient features of the 2HDM frameworks with a fourth-generation of fermions. (We will focus below on the quark sector, but a generalization to the leptonic sector is straightforward). Assuming a common, generic 2HDM potential, the phenomenology of 2HDMs is generically encoded in the texture of the Yukawa interaction Lagrangian. The simplest variant of a 2HDM with a fourth-generation of fermions can be constructed based on the so-called type-II 2HDM (which we denote hereafter by 2HDMII), in which one of the Higgs doublets couples only to up-type fermions, and the other only to down-type ones. This setup ensures the absence of tree-level flavor-changing neutral currents and is, therefore, widely favored when confronted with low-energy flavor data. The Yukawa terms for the quarks of the 2HDMII, extended to include the extra fourth-generation quark doublet, are

$$\mathcal{L}_Y = -\bar{Q}_L \Phi_d F_d d_R - \bar{Q}_L \tilde{\Phi}_u F_u u_R + \text{H.c.}, \tag{1}$$

where $f_{L(R)}$ ($f = u,\ d$) are left- (right-) handed fermion fields, $Q_L$ is the left-handed $SU(2)$ quark doublet, $F_d$, $F_u$ are general $4 \times 4$ Yukawa matrices in flavor space, and $\Phi_{d,u}$ are the Higgs doublets:

$$\Phi_i = \begin{pmatrix} \phi_i^+ \\ \frac{v_i + \phi_i^0}{\sqrt{2}} \end{pmatrix}, \qquad \tilde{\Phi}_i = \begin{pmatrix} \frac{v_i^* + \phi_i^{0*}}{\sqrt{2}} \\ -\phi_i^- \end{pmatrix}. \tag{2}$$

As mentioned above, motivated by the idea that the low-energy scalar degrees of freedom may be the composites of the heavy fourth-generation fermions, Bar-Shalom *et al.* [34] have constructed a new class of 2HDM's, named the 4G2HDM, that can effectively parameterize fourth-generation condensation by giving a special status to the fourth family of fermions. The possible viable variants of this approach can be parameterized as [34]

$$\begin{aligned} \mathcal{L}_Y = &-\bar{Q}_L(\Phi_\ell F_d \cdot (I - \mathcal{I}_d^{\alpha_d \beta_d}) + \Phi_h F_d \cdot \mathcal{I}_d^{\alpha_d \beta_d}) d_R \\ &- \bar{Q}_L(\tilde{\Phi}_\ell G_u \cdot (I - \mathcal{I}_u^{\alpha_u \beta_u}) + \Phi_h G_u \cdot \mathcal{I}_u^{\alpha_u \beta_u}) u_R + \text{H.c.}, \end{aligned} \tag{3}$$

where $\Phi_{\ell,h}$ are the two Higgs doublets, $I$ is the identity matrix, and $\mathcal{I}_q^{\alpha_q \beta_q}$ ($q = d,\ u$) are diagonal $4 \times 4$ matrices defined by $\mathcal{I}_q^{\alpha_q \beta_q} \equiv \text{diag}(0, 0, \alpha_q, \beta_q)$.

In particular, in the type-I 4G2HDM of Ref. [34] (which we will focus on below, and which will be denoted hereafter simply as the 4G2HDM), one sets $(\alpha_d, \beta_d, \alpha_u, \beta_u) = (0, 1, 0, 1)$, so that the "heavier" Higgs field ($\phi_h$) is assumed to couple only to the fourth-generation quarks, while the "lighter" Higgs field ($\phi_\ell$) is responsible for the mass generation of all other (lighter first-, second-, and third-generation) fermions.

The Yukawa interactions for these 4G2HDM models in terms of the physical states are given in Ref. [34]. For the lighter $CP$-even Higgs, it reads

$$\begin{aligned} \mathcal{L}(h q_i q_j) = \frac{g}{2 m_W} \bar{q}_i \Big\{ & m_{q_i} \frac{s_\alpha}{c_\beta} \delta_{ij} - \left( \frac{c_\alpha}{s_\beta} + \frac{s_\alpha}{c_\beta} \right) \\ & \cdot [m_{q_i} \Sigma_{ij}^q R + m_{q_j} \Sigma_{ji}^{q\star} L] \Big\} q_j h, \end{aligned} \tag{4}$$

where $\alpha$ is mixing angle in the $CP$-even neutral Higgs sector, $\tan\beta = v_h / v_\ell$ is the ratio between the vacuum expectation values of $\Phi_h$ and $\Phi_\ell$, and $\Sigma^d$, $\Sigma^u$ are new mixing matrices in the down- (up-) quark sectors, which

are obtained after diagonalizing the quark mass matrices. These matrices are key parameters of the model, which depend on the rotation (unitary) matrices of the right-handed down and up quarks, $D_R$ and $U_R$, and on whether $\alpha_q$ and/or $\beta_q$ are "turned on":

$$\Sigma^d_{ij} = \alpha_d D^\star_{R,3i} D_{R,3j} + \beta_d D^\star_{R,4i} D_{R,4j}, \quad (5)$$

$$\Sigma^u_{ij} = \alpha_u U^\star_{R,3i} U_{R,3j} + \beta_u U^\star_{R,4i} U_{R,4j}. \quad (6)$$

Thus, as opposed to "standard" 2HDMs, in the 4G2HDM some elements of $D_R$ and $U_R$ are physical and can, in principle, be measured in Higgs-fermion systems. In particular, inspired by the working assumption of the 4G2HDM and by the observed flavor pattern in the up- and down-quark sectors, it is shown in Ref. [34] that, for $(\alpha_d, \beta_d, \alpha_u, \beta_u) = (0, 1, 0, 1)$, the new mixing matrices $\Sigma^d$ and $\Sigma^u$ are expected to have the following form:

$$\Sigma^u = \begin{pmatrix} 0 & 0 & 0 & 0 \\ 0 & 0 & 0 & 0 \\ 0 & 0 & |\epsilon_t|^2 & \epsilon_t^\star\left(1 - \frac{|\epsilon_t|^2}{2}\right) \\ 0 & 0 & \epsilon_t\left(1 - \frac{|\epsilon_t|^2}{2}\right) & \left(1 - \frac{|\epsilon_t|^2}{2}\right) \end{pmatrix}, \quad (7)$$

and similarly for $\Sigma^d$ by replacing $\epsilon_t \to \epsilon_b$. The new parameters $\epsilon_t$ and $\epsilon_b$ are free parameters of the model that effectively control the mixing between the fourth-generation and the third-generation quarks. We therefore expect $\epsilon_b \ll \epsilon_t$, so that a natural choice for these parameters would be $\epsilon_b \sim \mathcal{O}(m_b/m_{b'})$ and $\epsilon_t \sim \mathcal{O}(m_t/m_{t'})$ (see also Ref. [34]). In what follows, we will thus set $\epsilon_b = 0$ and vary the $t$-$t'$ mixing parameter in the range $0 < \epsilon_t < 0.5$.

## III. 2HDM'S AND THE 125 GEV HIGGS SIGNALS

Clearly, once a new Higgs doublet is introduced, the phenomenology of the Higgs-particle production and decay becomes more complicated. In particular, the new Yukawa couplings depend on several more parameters (i.e., in the 4G2HDM, on $\epsilon_t$, $\epsilon_b$, $\tan\beta$, and $\alpha$), and the $CP$-even Higgs couplings to the $W$ and $Z$ bosons have extra prefactors of $\sin(\alpha\text{-}\beta)$ and $\cos(\alpha\text{-}\beta)$ (the pseudoscalar $A$ does not couple at tree level to the $W$ and the $Z$). As a result, the one-loop $h \to \gamma\gamma$ decay and the leading $gg \to h$ Higgs production mechanism can be significantly altered compared to their SM and SM4 values, depending on $\epsilon_t$, $\tan\beta$, $\alpha$, and on the fourth-generation fermion masses (i.e., assuming $\epsilon_b \ll \epsilon_t$, therefore setting $\epsilon_b = 0$ throughout our analysis). This is demonstrated in Fig. 1, where we plot the widths $\Gamma(h \to \gamma\gamma)$ and $\Gamma(h \to gg)$ as a function of these three parameters, setting $M_{4G} \equiv m_{t'} = m_{b'} = m_{l_4} = m_{\nu_4} = 400$ GeV. The dependence on $\tan\beta$ is depicted in a narrow range around $\tan\beta \sim 1$, for which the 4G2HDM is consistent with both EWPD [34] and the observed 125 GeV Higgs signals (see below).

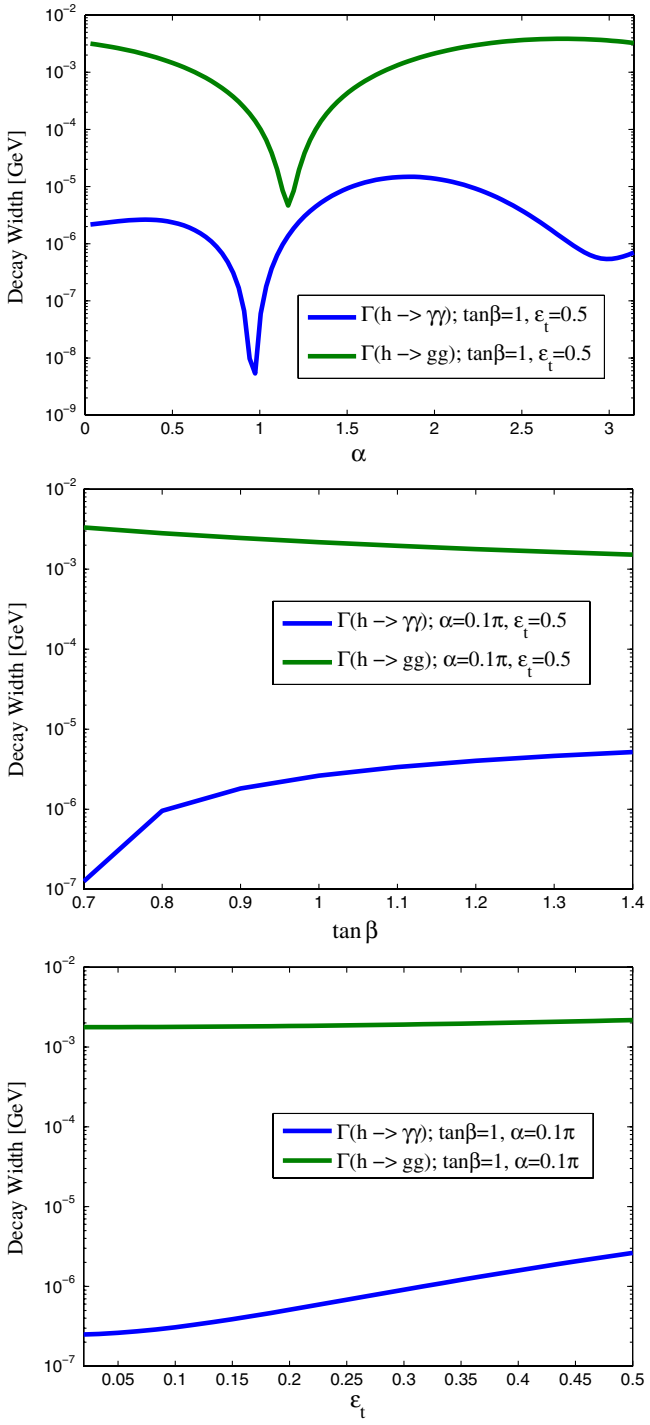


FIG. 1 (color online). $\Gamma(h \to \gamma\gamma)$ and $\Gamma(h \to gg)$ as a function of $\alpha$, $\tan\beta$ and $\epsilon_t$, for some representative values of these parameters (as indicated in the plots) and with $M_{4G} \equiv m_{t'} = m_{b'} = m_{l_4} = m_{\nu_4} = 400$ GeV.

We see that both $h \to \gamma\gamma$ and $h \to gg$ have a strong dependence on the Higgs mixing angle $\alpha$, while $h \to \gamma\gamma$ is

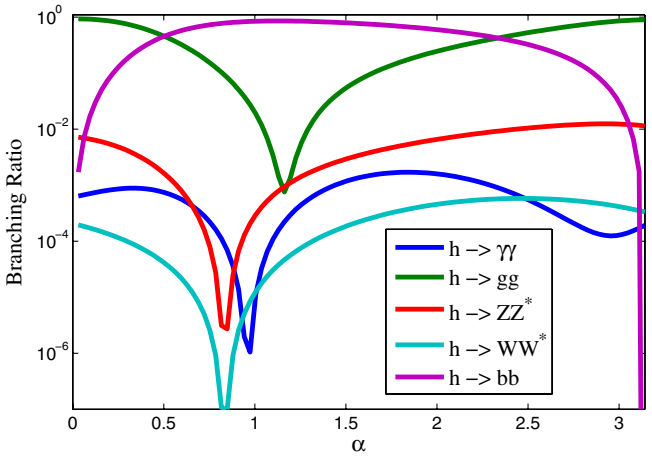


FIG. 2 (color online). The relevant branching ratios of $h$ in the 4G2HDM, as a function of $\alpha$, with $m_h = 125$ GeV, $M_{4G} = 400$ GeV, $\epsilon_t = 0.5$, and $\tan\beta = 1$.

also very sensitive to $\tan\beta$ and to the new $t$-$t'$ mixing parameter $\epsilon_t$, due to their role in the interference between the fermion loops and the $W$-boson loop. In Fig. 2, we further plot the various relevant branching ratios of a 125 GeV $h$ in the 4G2HDM, as a function of $\alpha$ for $\epsilon_t = 0.5$, $\tan\beta = 1$, and $M_{4G} = 400$ GeV.

Let us now turn to the recently reported LHC Higgs searches and the implications of the discovery of a 125 GeV Higgs-like particle on the 4G2HDM setup with a fourth-generation of fermions. The quantity that is usually being used for comparison between the LHC and Tevatron results and the expected signals in various models is the normalized cross section:

$$R_{XX}^{\text{Model(Obs)}} = \frac{\sigma(pp/p\bar{p} \to h \to XX)_{\text{Model(Obs)}}}{\sigma(pp/p\bar{p} \to h \to XX)_{\text{SM}}}. \quad (8)$$

For the observed ratios of cross sections; i.e., the signal strengths $R_{XX}^{\text{Obs}}$ and the corresponding errors $\sigma_{XX}$, we use the latest results as published in Refs. [1–3]:

(a) $VV \to h \to \gamma\gamma$: $2.2 \pm 1.4$ (taken from $\gamma\gamma + 2j$).
(b) $gg \to h \to \gamma\gamma$: $1.68 \pm 0.42$.
(c) $gg \to h \to WW^*$: $0.78 \pm 0.3$.
(d) $gg \to h \to ZZ^*$: $0.83 \pm 0.3$.
(e) $gg \to h \to \tau\tau$: $0.2 \pm 0.85$.
(f) $pp/p\bar{p} \to hW \to b\bar{b}W$: $1.8 \pm 1.5$.

The values given above are the result of a combination of the most recent data in each channel.[1] The uncertainties are calculated by treating the reported experimental uncertainties as statistical and assigning 15% theoretical uncertainty to the gluon fusion production mechanism, with 5% theoretical uncertainty on electroweak production mechanisms and the branching fractions [54]. One can easily notice that the channels with the highest sensitivity to the Higgs signals, and that contributed the most to the recent 125 GeV Higgs discovery, are $h \to \gamma\gamma$ and $h \to ZZ^*$, $WW^*$. In all other channels, the results are not conclusive, and at this time they are consistent with the background-only hypothesis at a level of less than $2\sigma$.

Clearly, a SM Higgs is ideally most consistent with $R_{XX}^{\text{Obs}} = 1$ in every channel, while in other models we expect some deviations in the various measured channels, depending on the parameters of the model and on the mass of the scalar candidate which should be compatible with the LHC results. Thus, the comparison to any given model can be performed using a $\chi^2$ fit:

$$\chi^2 = \sum_X \frac{\left(R_{XX}^{\text{Model}} - R_{XX}^{\text{Obs}}\right)^2}{\sigma_{XX}^2}, \quad (9)$$

where $\sigma_{XX}$ are the errors on the observed cross sections, and $R_{XX}^{\text{Model}}$ is the calculated normalized cross section in any given model. In particular, we take advantage of the fact that $\frac{\sigma(YY\to h)_{\text{Model}}}{\sigma(YY\to h)_{\text{SM}}} = \frac{\Gamma(h\to YY)_{\text{Model}}}{\Gamma(h\to YY)_{\text{SM}}}$, and calculate $R_{XX}^{\text{Model}}$ using

$$R_{XX}^{\text{Model}} = \frac{\Gamma(h \to YY)_{\text{Model}}}{\Gamma(h \to YY)_{\text{SM}}} \cdot \frac{\text{Br}(h \to XX)_{\text{Model}}}{\text{Br}(h \to XX)_{\text{SM}}}, \quad (10)$$

where $YY \to h$ is the Higgs production mechanism; i.e., either by gluon fusion $gg \to h$, vector boson fusion $WW/ZZ \to h$, or the associated Higgs-$W$ production $W^* \to hW$ at the Tevatron.

The Higgs signals in a 2HDM setup with a fourth-generation of fermions have already been discussed to some extent in the literature [44,45,47,48,55], but with no general picture of how these signals match all the observed Higgs cross sections reported above. Here, we try to quantify how well the 2HDM scenarios (where the lightest Higgs particle, $h$, has a mass of 125 GeV) fit all the available Higgs data, by calculating $\chi^2$ for all the relevant channels in two 2HDM realizations with four generations: the 2HDMII and the 4G2HDM (see Sec. II).

We use the latest version of Hdecay [56], with recent NLO contributions which also include the heavy fourth-generation fermions, where we have inserted all the relevant couplings of the 4G2HDM and the 2HDMII frameworks described in Sec. II. For the fourth-generation fermion masses involved in the loops of the decays $h \to VV$ (i.e., in the one-loop NLO corrections for the cases $h \to ZZ^*$, $WW^*$), we have used the approximation of a degenerate fourth-generation fermion sector, where we have tested below two representative cases: $m_{t'} = m_{b'} = m_{l_4} = m_{\nu_4} \equiv M_{4G} = 400$ and 600 GeV. [The effect of mass splittings between fourth-generation fermions on $\Gamma(h \to VV)$ is negligible]. It is important to note that, while the first case ($M_{4G} = 400$ GeV) is excluded for the SM4 [20], it is not necessarily excluded for the 4G2HDM, since in this model the decay patterns of $t'$ and $b'$ can have a

[1]We combine the results from the CMS and ATLAS experiments (for $pp/p\bar{p} \to hW \to b\bar{b}W$, we combine the results from CMS and Tevatron); in cases where the measured value was not explicitly given, we estimate it from the published plots.

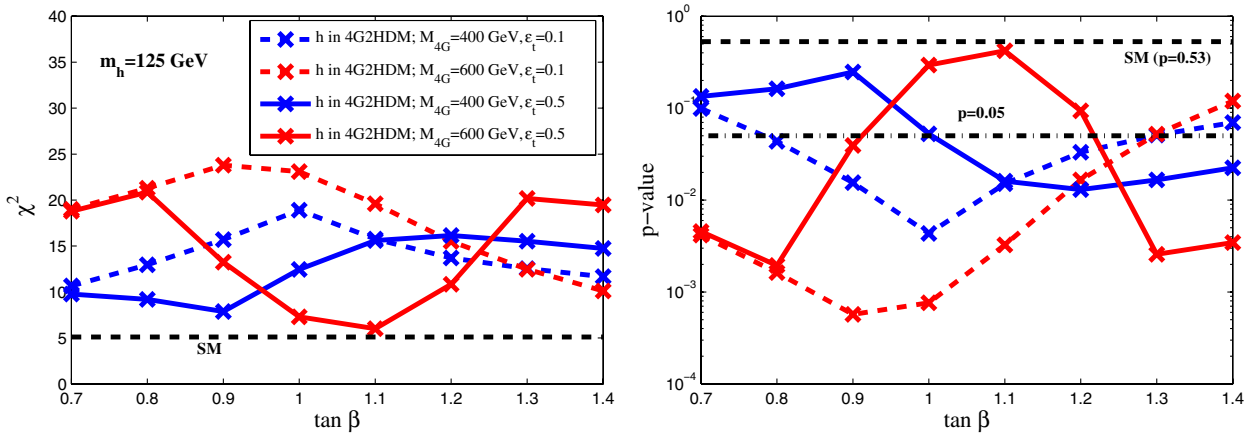


FIG. 3 (color online). $\chi^2$ (left plot) and $p$ values (right plot) as a function of $\tan\beta$ for the lightest 4G2HDM $CP$-even scalar $h$, with $m_h = 125$ GeV, $\epsilon_t = 0.1$ and 0.5, and $M_{4G} \equiv m_{t'} = m_{b'} = m_{l_4} = m_{\nu_4} = 400$ and 600 GeV. The value of the Higgs mixing angle $\alpha$ is the one which minimizes $\chi^2$ for each value of $\tan\beta$. The SM best fit is shown by the horizontal dashed line; the dash-dotted line in the right plot corresponds to $p = 0.05$ and serves as a reference line.

completely different topology, e.g., $\mathrm{BR}(t' \to th) \sim 1$, for which the current limits (which are based on the "standard" SM4 decays, $t' \to bW$ and $b' \to tW$) do not apply; see Ref. [53].

As mentioned earlier, we find that the simple SM4 case, with a 125 GeV Higgs is excluded to many $\sigma$'s when confronted with the Higgs search results. Also, as was already noted in Ref. [45] in the context of the "standard" 2HDMII (i.e., with four generations), we find that the simplest case of a light 125 GeV pseudoscalar $A$ of any 2HDM, with or without a fourth family, is not compatible with the Higgs data, irrespective of the fourth-generation fermion masses. In particular, the signals of the 125 GeV Higgs decaying into a pair of vector bosons, $h \to ZZ$ and $h \to WW$, excludes this possibility due to the absence of tree-level $AZZ$ and $AWW$ couplings. We therefore focus below only on the case where the observed 125 GeV Higgs-like particle is the lighter $CP$-even Higgs, $h$.

We plot in Fig. 3 the resulting $\chi^2$ and $p$ values in the 4G2HDM case (combining all six reported Higgs decay channels above), with $m_h = 125$ GeV, $M_{4G} = 400$ and 600 GeV, $\epsilon_t = 0.1$ and 0.5, and with $0.7 < \tan\beta < 1.4$. (This range is allowed by EWPD and flavor physics in the 2HDM fourth-generation setups; see Refs. [34,52].) The value of the Higgs mixing angle $\alpha$ is that which minimizes the $\chi^2$ for each value of $\tan\beta$. The SM best fit is also shown in the plot. In Fig. 4, we further plot the resulting $\chi^2$ and $p$ values as a function of $\tan\beta$, this time minimizing for each value of $\tan\beta$ with respect to both $\alpha$ and $\epsilon_t$ (in the 4G2HDM case). For comparison, we also show in Fig. 4 the $\chi^2$ and $p$ values for a 125 GeV $h$ in the 2HDMII with a fourth-generation, and in the SM.

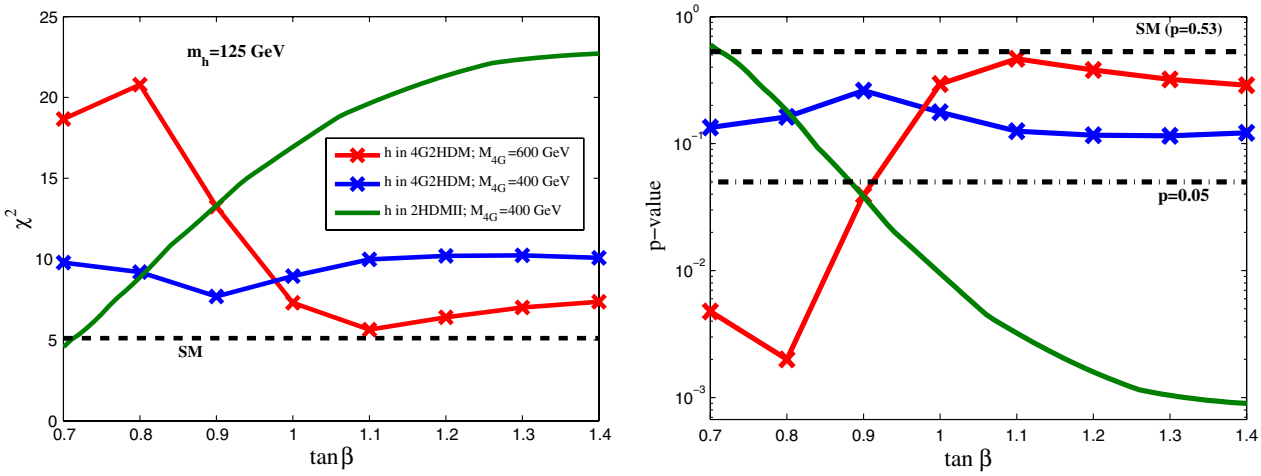


FIG. 4 (color online). Same as Fig. 3, where here we minimize with respect to both $\epsilon_t$ and $\alpha$ for each value of $\tan\beta$. Also shown are the $\chi^2$ and $p$ values for a 125 GeV Higgs in the SM and in the type-II 2HDM with a fourth-generation of fermions (denoted by 2HDMII).

TABLE I. Six representative best-fitted sets of values for $\{\tan\beta, \alpha, \epsilon_t, M_{4G}\}$ in the 4G2HDM, corresponding to points on the best-fitted 4G2HDM curves shown in Fig. 4.

| Point # | $\tan\beta$ | $\alpha$ | $\epsilon_t$ | $M_{4G}$ [GeV] |
|---|---|---|---|---|
| P1 | 0.7 | $0.09\pi$ | 0.5 | 400 |
| P2 | 0.7 | $0.51\pi$ | 0.433 | 600 |
| P3 | 1.0 | $0.1\pi$ | 0.42 | 400 |
| P4 | 1.0 | $0.08\pi$ | 0.5 | 600 |
| P5 | 1.3 | $0.11\pi$ | 0.3 | 400 |
| P6 | 1.3 | $0.07\pi$ | 0.33 | 600 |

Looking at the $p$ values in Figs. 3 and 4 (which "measure" the extent to which a given model can be successfully used to interpret the Higgs data in all the measured decay channels), we see that the $h$ of the 4G2HDM with $\tan\beta \sim \mathcal{O}(1)$ and $M_{4G} = 400$–$600$ GeV is a good candidate for the recently observed 125 GeV Higgs, giving a fit comparable to the SM fit. The "standard" 2HDMII setup with $M_{4G} = 400$ and 600 GeV (the case of $M_{4G} = 600$ GeV is not shown in the plot) is also found to be consistent with the Higgs data in a narrower range of $\tan\beta \lesssim 0.9$. We find that the fit favors a large $t$-$t'$ mixing parameter $\epsilon_t$, implying $\mathrm{BR}(t' \to th) \sim \mathcal{O}(1)$, which completely changes the $t'$ decay pattern [34], and therefore significantly relaxes the current bounds on $m_{t'}$ [53]. This can be seen in Table I, where we list six representative sets of best-fitted values (to be used in the plots below) for $\{\tan\beta, \alpha, \epsilon_t, M_{4G}\}$ in the 4G2HDM that correspond to points on the best-fitted 4G2HDM curves shown in Fig. 4.

In Fig. 5, we further test the goodness of fit for the 125 GeV $h$ of the 4G2HDM, where, in addition to the Higgs results, we explicitly impose the constraints on the 4G2HDM parameter space from EWPD (from the $S$ and $T$ parameters and from $Z \to b\bar{b}$) using the results in Refs. [34,52]. Evidently, our conclusions above do not change after adding the EWPD constraints to the analysis.

Finally, we note that we have also tested the three-generation type-II 2HDM and found that its lightest $CP$-even Higgs is also a good candidate for the observed 125 GeV Higgs particle, giving a fit which is also comparable to the SM fit for $\tan\beta \sim \mathcal{O}(1)$.

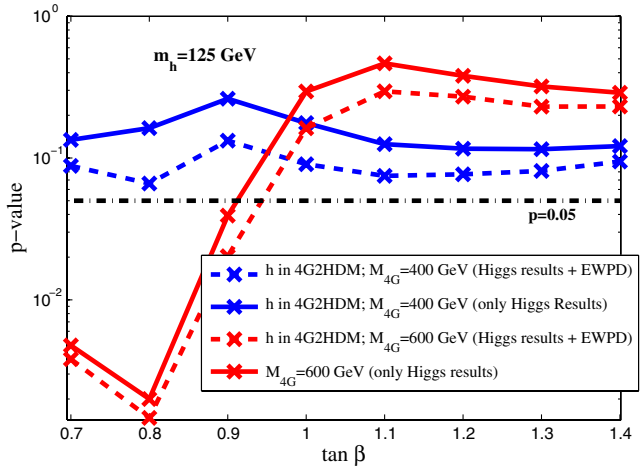


FIG. 5 (color online). A comparison between the $p$ values for the compatibility of the 125 GeV $h$ of the 4G2HDM with the Higgs search results, with (dashed lines) and without (solid lines) imposing the constraints from EWPD as given in Refs. [34,52]. The dash-dotted line corresponds to $p = 0.05$. Here also, the parameters $\alpha$ and $\epsilon_t$ are chosen by a minimization of $\chi^2$.

## IV. HIGGS PHENOMENOLOGY IN THE 4G2HDM

In Fig. 6, we plot the individual pulls and the signal strengths for the various measured channels, $(R_{XX}^{\mathrm{4G2HDM}} - R_{XX}^{\mathrm{Obs}})/\sigma_{XX}$ and $R_{XX}^{\mathrm{4G2HDM}}$, respectively, as a function of $\tan\beta$, for the above best-fitted 4G2HDM curve with $M_{4G} = 400$ GeV. We see that appreciable deviations from the SM are expected in the channels $gg \to h \to \tau\tau$, $VV \to h \to \gamma\gamma$, and $hV \to bbV$. In particular, the most

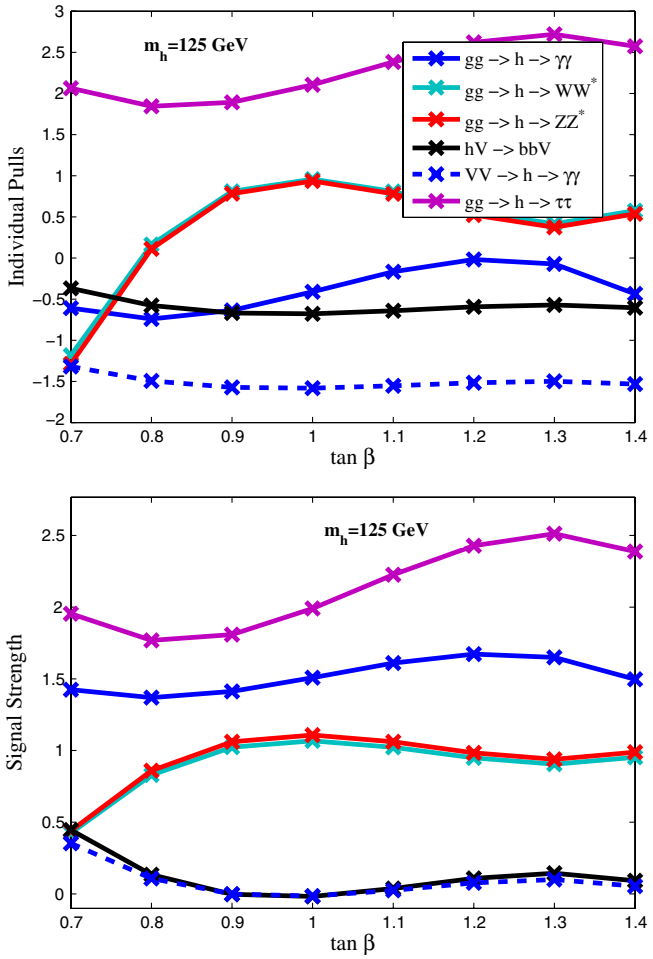


FIG. 6 (color online). The individual pulls $\frac{(R_{XX}^{\mathrm{Model}} - R_{XX}^{\mathrm{Obs}})}{\sigma_{XX}}$ (upper plot), and the signal strengths $R_{XX}^{\mathrm{Model}}$ (lower plot), in the different channels, that correspond to the best-fitted 4G2HDM curve with $m_h = 125$ GeV and $M_{4G} = 400$ GeV, shown in Fig. 4.

notable effects are about a $1.5\sigma$ deviation (from the observed value) in the vector boson fusion diphoton channel $VV \to h \to \gamma\gamma$ and a 2–$2.5\sigma$ deviation in the $gg \to h \to \tau\tau$ channel. The deviations in these channels are in fact a prediction of the 4G2HDM strictly based on the current Higgs data, which could play a crucial role as data with higher statistics become available. They can be understood as follows: the channels that dominate the fit (i.e., having a higher statistical significance due to their smaller errors) are $gg \to h \to \gamma\gamma, ZZ^*, WW^*$. Thus, since the $gg \to h$ production vertex is generically enhanced by the $t'$, $b'$ loops, the fit then searches for values of the relevant 4G2HDM parameters which decrease the $h \to \gamma\gamma, ZZ^*, WW^*$ decays by the appropriate amount. This, in turn, leads to an enhanced $gg \to h \to \tau\tau$ (i.e., due to the enhancement in the $gg \to h$ production vertex) and to a decrease in the $VV \to h \to \gamma\gamma$ and $p\bar{p}/pp \to W \to hW \to bbW$ channels, which are independent of the enhanced $ggh$ vertex but are sensitive to the decreased $VVh$ one. It is important to note that some of the characteristics of these "predictions" can change with more data collected.

We conclude with the implications of the above results for the other two neutral scalars of the 4G2HDM. For the heavier $CP$-even neutral Higgs, $H$, we consider its decays to $ZZ$ and $WW$, which are currently the most sensitive channels in which searches for a heavy SM Higgs were performed at the LHC. A useful approximation of the expected exclusion range on $m_H$ can be performed by comparing the calculated signal strengths,

$$R^H_{ZZ/WW} \equiv \frac{\sigma(pp \to H \to ZZ/WW)_{\text{4G2HDM}}}{\sigma(pp \to H \to ZZ/WW)_{\text{SM}}}, \qquad (11)$$

to the observed/measured values of this quantity; i.e., to $R^{\text{Obs}}_{ZZ/WW}$. (Note that in the 4G2HDM we find $R^H_{WW} \sim R^H_{ZZ}$ for $m_H > 2m_W$). In Fig. 7, we plot $R^H_{ZZ}$ as a function of $m_H$ for the six best-fitted points of the relevant 4G2HDM parameter space, given in Table I. We also show in Fig. 7 an approximate exclusion line for $R_{ZZ}$; i.e., for the observed signal strength $R^{\text{Obs}}_{ZZ}$, which we have extracted from the most recent CMS exclusion plot in this channel (see Ref. [57]) and which is currently the most stringent observed exclusion limit for a heavy Higgs with a mass $\gtrsim$ 200 GeV. We see that $m_H \lesssim 600$ GeV is excluded by the current data in the $H \to ZZ$ channel for points P1, P2, P3 and P5 (i.e., $R^H_{ZZ}(P1, P2, P3, P5) > R^{\text{Obs}}_{ZZ}$ for $m_H \lesssim$ 600 GeV), while for points P4 and P6 $m_H \gtrsim 500$ GeV is allowed.

The current CMS and ATLAS Higgs data in the $ZZ$ and $WW$ channels are not sensitive to the pseudoscalar $A$, due to the absence of tree-level $AZZ$ and $AWW$ couplings (and due to the smallness of the corresponding $AZZ$ and $AWW$ one-loop couplings [58]). Therefore, the only relevant search channels which are currently sensitive to $A$ decays are $A \to \gamma\gamma$ and $A \to \tau\tau$, for which a search for the Higgs was performed up to a Higgs mass slightly below $2m_W$ by both CMS and ATLAS. Defining the signal strengths for the $A$ signals as

$$R^A_{\tau\tau/\gamma\gamma} \equiv \frac{\sigma(pp \to A \to \tau\tau/\gamma\gamma)_{\text{4G2HDM}}}{\sigma(pp \to H \to \tau\tau/\gamma\gamma)_{\text{SM}}}, \qquad (12)$$

we plot in Figs. 8 and 9 $R^A_{\tau\tau}$ and $R^A_{\gamma\gamma}$, respectively, as functions of $m_A$ (we assume that $m_A > m_h$), for points P1–P6 of Table I. Here also, we plot the existing approximate exclusion lines $R^{\text{Obs}}_{\tau\tau}$ and $R^{\text{Obs}}_{\gamma\gamma}$, based on the most recent CMS analysis, which currently gives the most stringent limits in these two channels [59,60]. We see that a pseudoscalar as light as 130 GeV is allowed by the current data, e.g., for points P1 and P2.

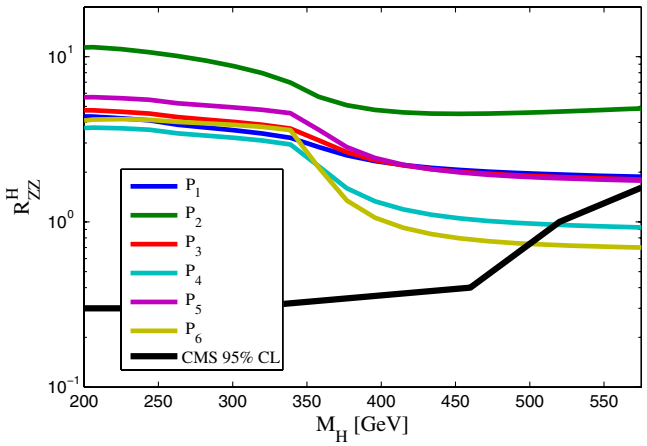


FIG. 7 (color online). The signal strength in the $H \to ZZ$ channel for the six best-fitted sets of values in Table I. Also shown is the approximate observed CMS limit on the signal strength in the $ZZ$ channel; i.e., $R^{\text{Obs}}_{ZZ}$ (see also the text).

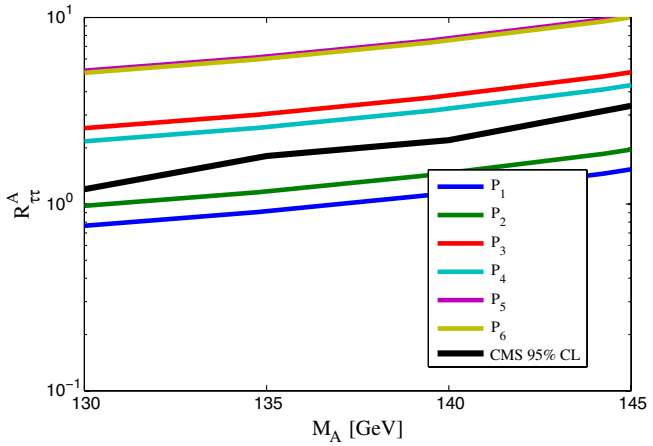


FIG. 8 (color online). The signal strengths in the $A \to \tau\tau$ channel for the six best-fitted sets of values in Table I. Also shown is the approximate observed CMS limit on signal strengths in the $\tau\tau$ channel; i.e., $R^{\text{Obs}}_{\tau\tau}$ (see also the text).

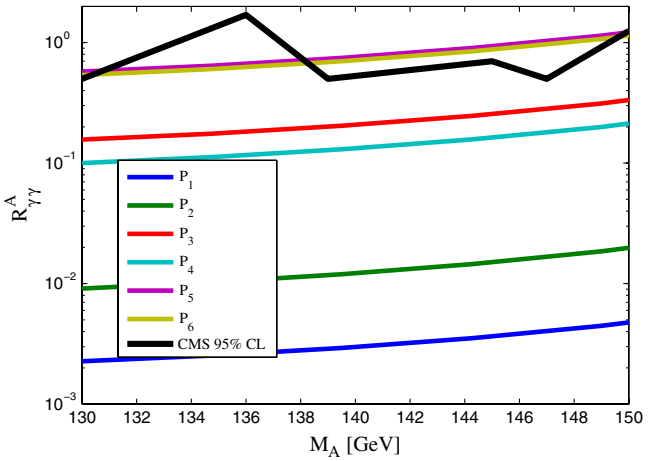


FIG. 9 (color online). The signal strengths in the $A \to \gamma\gamma$ channel, for the 6 best-fitted sets of values in Table I. Also shown is the approximate observed CMS limit on signal strengths in the $\gamma\gamma$ channel; i.e., $R^{\mathrm{Obs}}_{\gamma\gamma}$ (see also the text).

## V. SUMMARY

We have studied the recently measured Higgs signals in the framework of a specific 2HDM with a fourth-generation of fermions (the 4G2HDM suggested in Ref. [34]), designed and motivated by the possibility that the sub-TeV Higgs particles are condensates of the heavy fourth-generation fermions, which are therefore viewed as the agents of dynamical electroweak symmetry breaking.

We find that the lightest *CP*-even Higgs state of this model, $h$, is a good candidate for the recently discovered 125 GeV Higgs signals in all the measured channels, within a large portion of the 4G2HDM-allowed parameter space, which is consistent with the current bounds from EWPD. In particular, for typical fourth-generation fermion masses in the range $M_{4G} = 400$–$600$ GeV, $\tan\beta \sim \mathcal{O}(1)$, and a large $t$-$t'$ mixing (the parameter $\epsilon_t$ predicted by the model), the lightest 4G2HDM Higgs gives a good overall fit to the current 125 GeV Higgs data—roughly comparable to the SM fit.

For these values of the 4G2HDM parameter space—in particular, with $\epsilon_t \sim 0.5$—the flavor-changing $t'$ decay $t' \to th$ dominates with $\mathrm{BR}(t' \to th) \sim 1$, leading to different $pp \to t'\bar{t}'$ signatures (than the simple SM4) that can be searched for at the LHC using the methods suggested in Ref. [53].

We also find that, based on the current Higgs data, the 4G2HDM predicts large deviations from the SM in the channels $pp \to h \to \tau\tau$, $VV \to h \to \gamma\gamma$, and $hV \to Vbb$, which remain to be tested with more data.

Finally, the heavier *CP*-even Higgs state, $H$, is found to be excluded in this model up to ~500 GeV, while the pseudoscalar Higgs state, $A$, can be as light as 130 GeV and can, therefore, be discovered (or ruled out in this small mass range) with more data collected in the $pp \to \tau\tau$, $\gamma\gamma$ channels.

## ACKNOWLEDGMENTS

We want to thank Michael Chanowitz for useful correspondence. S. B. S. and M. G. acknowledge research support from Technion. G. E. thanks R. Godbole and S. Vempati for hospitality and discussions. The work of A. S. was supported in part by U.S. DOE Contract No. DE-AC02-98CH10886(BNL).

[1] S. Chatrchyan *et al.* (CMS Collaboration), Phys. Lett. B **716**, 30 (2012); see also J. Incandela, in The ICHEP, Melbourne, Australia, 2012 (unpublished).
[2] G. Aad *et al.* (ATLAS Collaboration), Phys. Lett. B **716**, 1 (2012); see also R. Hawkings, in The ICHEP, Melbourne, Australia, 2012 (unpublished).
[3] Tevatron New Phenomena, Higgs Working Group (TEVNP), CDF, and D0 Collaborations, arXiv:1203.3774.
[4] P. H. Frampton, P. Q. Hung, and M. Sher, Phys. Rep. **330**, 263 (2000).
[5] B. Holdom, W. S. Hou, T. Hurth, M. L. Mangano, S. Sultansoy, and G. Unel, PMC Phys. A **3**, 4 (2009).
[6] For older literature on the SM4, see *Proceedings of the First International Symposiums on the fourth family of quarks and leptons, Santa Monica, CA, 1987*, edited by D. Cline and A. Soni, Annals of New York Academy of Science Vol. 517 (New York Academy of Sciences, New York, 1987); and *Proceedings of the Second International Symposiums on the fourth family of quarks and leptons, Santa Monica, CA, 1989*, edited by D. Cline and A. Soni, Annals of New York Academy of Science, Vol. 578 (New York Academy of Sciences, New York, 1990).
[7] For a review of the implications of stable quarks of the fourth-generation on cosmology, astrophysics and accelerator physics, see K. Belotsky, M. Khlopov, and K. Shibaev, arXiv:0806.1067 and references therein.
[8] B. Holdom, Phys. Rev. Lett. **57**, 2496 (1986); **58**, 177(E) (1987); W. A. Bardeen, C. T. Hill, and M. Lindner, Phys. Rev. D **41**, 1647 (1990); S. F. King, Phys. Lett. B **234**, 108 (1990); C. Hill, M. Luty, and E. A. Paschos, Phys. Rev. D **43**, 3011 (1991); P. Q. Hung and G. Isidori, Phys. Lett. B **402**, 122 (1997).
[9] B. Holdom, J. High Energy Phys. 08 (2006) 076.
[10] P. Q. Hung and Chi Xiong, Nucl. Phys. **B848**, 288 (2011).
[11] Y. Mimura, W. S. Hou, and H. Kohyama, arXiv:1206.6063.
[12] W. S. Hou, Chin. J. Phys. (Taipei) **47**, 134 (2009); arXiv:0810.3396; S. W. Ham, S. K. Oh, and D. Son, Phys. Rev. D **71**, 015001 (2005); G. W. S. Hou, Int. J. Mod. Phys. D **20**, 1521 (2011).

[13] S. W. Ham, S. K. Oh, and D. Son, Phys. Rev. D **71**, 015001 (2005); R. Fok and G. D. Kribs, Phys. Rev. D **78**, 075023 (2008).

[14] A. Soni, A. K. Alok, A. Giri, R. Mohanta, and S. Nandi, Phys. Lett. B **683**, 302 (2010).

[15] A. Soni, A. K. Alok, A. Giri, R. Mohanta, and S. Nandi, Phys. Rev. D **82**, 033009 (2010).

[16] A. J. Buras, B. Duling, T. Feldmann, T. Heidsieck, C. Promberger, and S. Recksiegel, J. High Energy Phys. 09 (2010) 106.

[17] A. J. Buras, B. Duling, T. Feldmann, T. Heidsieck, C. Promberger, and S. Recksiegel, J. High Energy Phys. 07 (2010) 094.

[18] W.-S. Hou, M. Nagashima, and A. Soddu, Phys. Rev. D **76**, 016004 (2007); M. Bobrowski, A. Lenz, J. Riedl, and J. Rohrwild, Phys. Rev. D **79**, 113006 (2009); V. Bashiry, N. Shirkhanghah, and K. Zeynali, Phys. Rev. D **80**, 015016 (2009); W. S. Hou and C. Y. Ma, Phys. Rev. D **82**, 036002 (2010); O. Eberhardt, A. Lenz, and J. Rohrwild, Phys. Rev. D **82**, 095006 (2010); S. Nandi and A. Soni, Phys. Rev. D **83**, 114510 (2011); A. K. Alok, A. Dighe, and D. London, Phys. Rev. D **83**, 073008 (2011); D. Choudhury and D. K. Ghosh, J. High Energy Phys. 02 (2011) 033; R. Mohanta and A. K. Giri, Phys. Rev. D **85**, 014008 (2012); A. Ahmed, I. Ahmed, M. J. Aslam, M. Junaid, M. A. Paracha, and A. Rehman, Phys. Rev. D **85**, 034018 (2012).

[19] M. S. Chanowitz, Phys. Rev. D **82**, 035018 (2010); **79**, 113008 (2009).

[20] M. M. H. Luk (CMS Collaboration), arXiv:1110.3246v2; S. Chatrchyan *et al.* (CMS Collaboration), Phys. Lett. B **716**, 103 (2012); G. Aad *et al.* (ATLAS Collaboration), Phys. Rev. Lett. **109**, 032001 (2012); S. Chatrchyan *et al.* (CMS Collaboration), J. High Energy Phys. 05 (2012) 123.

[21] ATLAS Collaboration, ATLAS Conference Note No. 2011-135; S. Chatrchyan *et al.* (CMS Collaboration), Phys. Lett. B **710**, 26 (2012).

[22] K. Nakamura *et al.* (Particle Data Group), J. Phys. G **37**, 075021 (2010).

[23] O. Eberhardt, G, Herbert, H. Lacker, A. Lenz, A. Menzel, U. Nierste, and M. Wiebusch, Phys. Rev. D **86**, 013011 (2012).

[24] A. Djouadi and A. Lenz, Phys. Lett. B **715**, 310 (2012).

[25] E. Kuflik, Y. Nir, and T. Volanski, arXiv:1204.1975.

[26] O. Eberhardt, A. Lenz, A. Menzel, U. Nierste, and M. Wiebusch, Phys. Rev. D **86**, 074014 (2012).

[27] G. D. Kribs, T. Plehn, M. Spannowsky, and T. M. P. Tait, Phys. Rev. D **76**, 075016 (2007).

[28] G. Passarino, C. Sturm, and S. Uccirati, Phys. Lett. B **706**, 195 (2011).

[29] A. Denner, S. Dittmaier, A. Mück, G. Passarino, M. Spira, C. Sturm, S. Uccirati, and M. M. Weber, Eur. Phys. J. C **72**, 1992 (2012).

[30] G. Guo, B. Ren, and X.-G. He, arXiv:1112.3188.

[31] O. Eberhardt *et al.*, arXiv:1209.1101.

[32] M. A. Luty, Phys. Rev. D **41**, 2893 (1990).

[33] M. Hashimoto and V. A. Miransky, Phys. Rev. D **81**, 055014 (2010).

[34] S. Bar-Shalom, S. Nandi, and A. Soni, Phys. Rev. D **84**, 053009 (2011).

[35] P. Q. Hung and C. Xiong, Nucl. Phys. **B847**, 160 (2011).

[36] P. Q. Hung and C. Xiong, Phys. Lett. B **694**, 430 (2011).

[37] K. Ishiwata and M. B. Wise, Phys. Rev. D **83**, 074015 (2011).

[38] A. E. C. Hernandez, C. O. Dib, H. N. Neill, and A. R. Zerwekh, J. High Energy Phys. 02 (2012) 132.

[39] G. Burdman and L. Da Rold, J. High Energy Phys. 12 (2007) 086.

[40] G. Burdman, L. Da Rold, O. Eboli, and R. D. Matheus, Phys. Rev. D **79**, 075026 (2009); G. Burdman, L. de Lima, and R. D. Matheus, Phys. Rev. D **83**, 035012 (2011).

[41] E. De Pree, G. Marshall, and M. Sher, Phys. Rev. D **80**, 037301 (2009).

[42] H.-S. Lee and A. Soni, arXiv:1206.6110.

[43] M. Sher, Phys. Rev. D **61**, 057303 (2000).

[44] W. Bernreuther, P. Gonzales, and M. Wiebusch, Eur. Phys. J. C **69**, 31 (2010).

[45] J. F. Gunion, arXiv:1105.3965.

[46] G. Burdman, C. Haluch, and R. Matheus, J. High Energy Phys. 12 (2011) 038.

[47] X.-G. He and G. Valencia, Phys. Lett. B **707**, 381 (2012).

[48] N. Chen and H. He, J. High Energy Phys. 04 (2012) 062.

[49] S. Litsey and M. Sher, Phys. Rev. D **80**, 057701 (2009).

[50] S. Dawson and P. Jaiswal, Phys. Rev. D **82**, 073017 (2010).

[51] R. C. Cotta, J. L. Hewett, A. Ismail, M.-P. Le, and T. G. Rizzo, Phys. Rev. D **84**, 075019 (2011).

[52] S. Bar-Shalom, M. Geller, S. Nandi, and A. Soni, arXiv:1208.3195, a review to appear in a special issue of Advances in High Energy Physics (AHEP) on Very Heavy Quarks at the LHC.

[53] M. Geller, S. Bar-Shalom, and G. Eilam, Phys. Lett. B **715**, 121 (2012).

[54] J. Campbell, in ICHEP, Melbourne, Australia, 2012 (unpublished).

[55] L. Bellantoni, J. Erler, J. Heckman, and E. Ramirez-Homs, Phys. Rev. D **86**, 034022 (2012).

[56] A. Djouadi, J. Kalinowski, and M. Spira, Comput. Phys. Commun. **108**, 56 (1998).

[57] CMS Collaboration, CMS Report No. CMS-PAS-HIG-12-016, available on the CERN CDS information server.

[58] See e.g., J. F. Gunion, H. E. Haber, and C. Kao, Phys. Rev. D **46**, 2907 (1992).

[59] CMS collaboration, CMS Report No. CMS-PAS-HIG-12-018, available on the CERN CDS information server.

[60] CMS collaboration, CMS Report No. CMS-PAS-HIG-12-015, available on the CERN CDS information server.